Optimization of Graphite-Epoxy Cylindrical Shell Panels with Cutout and Stiffeners under Vibration – Finite Element based Taguchi Analysis

Sudip Kr. Halder[1], Anirban Mitra[1] and Sarmila Sahoo[2*]

[1]*Department of Mechanical Engineering, Jadavpur University, Kolkata, India*
[2]*Department of Civil Engineering, Heritage Institute of Technology, Kolkata, India*
*Corresponding author: sarmila.sahoo@gmail.com; sarmila.sahoo@heritageit.edu

Received 27/01/2026; accepted 20/06/2026
https://doi.org/10.4152/pea.2027450603

Abstract
Graphite-epoxy cylindrical shell panels find widespread application in engineering structures. Various functional requirements necessitate use of cutouts and stiffeners in shell panels. To evade resonating damage, natural frequency of such structures should be optimized. The present study obtained natural frequency of cylindrical shell panels with cutout using finite element analysis, and optimized it based on Taguchi analysis for different edge constraints. Numerical study was performed following L27 Taguchi orthogonal design, where fiber direction, thickness ratio, degree of orthotropy and location of cutout were considered as design variables. Shallowness of the shell panel expressed in terms of width/thickness ratio influenced the fundamental frequency most followed by degree of orthotropy.

Keywords: cutout; cylindrical shell panel; free vibration; laminated composite; stiffener; Taguchi optimization.

Introduction•

Since laminated composite shells find extensive application in engineering structural components, researchers take keen interest in studying their behavior. In comparison to common metallic materials used in structures, laminated composites are advantageous in terms of higher specific strength and stiffness, enhanced resistance to environmental toxic attacks, longer life span and the ability to engineer properties as desired. In recent times, composite manufacturing technology has developed significantly due to availability of advanced technology like 3D printers, which has led to an overwhelming usage of composite shell panels in diverse applications, such as aerospace, automobile, marine, civil and mechanical structures. Cylindrical shell panels are commonly used as load-bearing structures in such applications. In order to yield higher strength, better stiffness and proper buckling characteristics, these shell panels are designed with stiffeners.

•The abbreviations list is in page 724.

Composite cylindrical shells provide higher rigidity compared to plates, due to their curved geometry. Hence, large unsupported roofs in airports, malls and parking lots can be made with these shell panels. This essentially reduces material consumption and simultaneously provides decorative design. Moreover, cylindrical shell panels can be fabricated easily since these singly ruled surfaces can be generated by straight shuttering.

Shell panels are normally thin-walled structures that show better performance when coupled with stiffeners, particularly in cutout borne structures. Moreover, they are very responsive to imperfections due to the presence of the cutouts. Normally, flexural stiffness and strength can be improved by providing higher wall thickness. However, the same stiffness and strength is achievable with stiffeners, hence using lesser amount of material. Stiffeners provide extra rigidity in such weight-sensitive applications. Instead of stiffening the complete structure, stiffeners may be employed locally around the cutouts. Cutouts often become essential in panels to meet different practical requirements like passage of light, convenience for inspection and maintenance, ventilation and, at times, adjustment of resonating frequency. The presence of cutouts, their size and positioning are decided by various technical and operational needs. Thus, it becomes essential to accurately regulate structural vibration response for proper design and effective applications. This paper aims at optimizing vibratory response of laminated cylindrical shells with stiffeners and cutouts for various practical edge constraints.

Natural frequencies of shell panels may become occupied in resonant vibrations. Natural frequencies need to be ascertained for fail-safe design of the structure against vibration [1, 2]. Vibratory characteristics of cylindrical shell structures have been elaborately studied over the years. Ritz method has been used by [3] to consider dynamic behavior of cantilever shallow cylindrical shells of rectangular shape in a plan view. A generalized analytical approach for obtaining the dynamic behavior of cylindrical shell with common edge supports was presented by [4]. Results have been obtained by [5] for free vibration of full cylindrical shells under simple supports using an updated shear deformable element. A higher order shear deformation theory has been considered by [6] to obtain dynamic behavior of thick cylindrical shallow shells. Rayleigh-Ritz variational approach has been used by [7] to analytically study free vibration behavior of thin cylindrical shells. Wave propagation method was also used by [8, 9] for dynamic analysis of such shells. Some studies [10, 11] have with static and dynamic responses of such panels in the presence of cutouts. Free vibration for panels with concentric cutout has been considered by [12]. Free vibration of composite cylindrical shells with cutouts having varied size and positioning has also been considered using finite element (FE) approach [13]. Very recently, differential transform technique has been applied to consider free vibration of cylindrical shell panels with cutouts [14]. An optimization method to obtain innovative stiffening layouts for cylindrical shell structures has been proposed by [15]. First-order shear deformation theory has been combined by [16] with spectral-Tchebychev technique to analyze free

vibration characteristics of stepped and stiffened composite cylindrical shells. Vibration of composite panel in the presence of centrally located square cutout was studied by [17] using 'Multi-domain Generalized Differential Quadrature' method. Parametric resonance of a three-layered cylindrical shell has been considered by [18]. A FE-based vibration study of cut-out borne stiffened composite cylindrical shells has been presented by [19].
Eight node isoparametric shell elements coupled with three node beam elements are used to study higher mode vibration behavior. In a recent study, [20] has considered optimal design of cylindrical composite shells subject to compression loads. Fifth order shear deformation theory was used by [21] to consider bending of laminated composite cylindrical shells. Buckling optimization [22] and non-linear vibration suppression [23] of such shells have also been recently reported.
Vibration frequencies of shell panels are dependent on many factors such as shell geometry, material properties, stiffener attributes, cutouts and boundary conditions, as shown in Fig. 1.

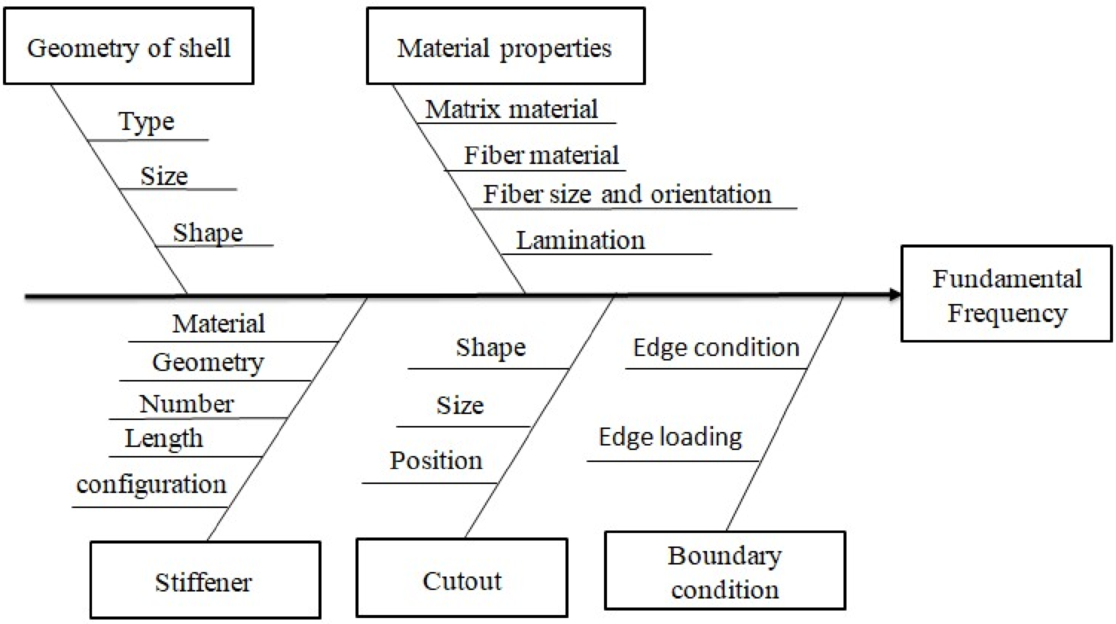

Figure 1: Fishbone diagram for factors affecting fundamental frequency of shell panel.

Thus, obtaining an appropriate combination of these factors that yields maximum fundamental frequency for a composite cylindrical shell with cutout is a challenging problem. In order to evade any resonating damage due to seismic oscillations and other natural disturbances, higher fundamental is desirable.
Detailed review of available literature reveals few studies on optimization of vibration frequency of composite cylindrical panels. The present study couples Taguchi approach [24] with numerical procedures based on FE formulation to obtain the appropriate amalgamation of multiple design variables to yield the maximum natural frequency of the shell panel. Accordingly, it was obtained a proper combination of design factors that yields maximum natural frequency of

vibration. Analysis of variance (ANOVA) [25] identifies dominant controlling parameters and level of dominance of their interactions.

Taguchi method

Taguchi approach is a useful method that analyses total design space based on orthogonal array (OA). OA supports lowered variation for the experiments with an optimum grouping of controlling factors. It thus utilizes a reduced number of experimental runs to judge all controlling factors and interaction between them. For achieving optimum combination of factors, it employs the design of experiments (DOE) technique using suitable OA. DOE technique is useful as it allows the scrutiny of the effect of design parameters on the response variable. It reduces the need for conducting numerous tests to be performed during the study. In the current study, numerical experiments were undertaken using Finite Element (FE) Analysis to find out the free vibration frequency of the composite stiffened cylindrical shell panel with cutout. Taguchi approach adopts signal-to-noise ratio (S/N) to quantify the quality characteristics deviating from preferred values. S/N ratio is expressed as the ratio of mean value of response to standard deviation of noise value. It is utilized to determine relative ranks of input design factors, considering three categories of quality characteristics: higher-the-better, nominal-the-best and smaller-the-better. Optimal condition is determined by identifying the grouping of factor levels that produces highest value of S/N ratio. Since in this study, maximization of fundamental frequency was the goal, a higher-the-better criterion was chosen. Furthermore, ANOVA was conducted to identify considerable factors. By combining S/N ratio analysis and ANOVA, appropriate settings for controlling factors that optimize response function were determined. Finally, confirmation test validated optimal factor settings so obtained. Flowchart of Taguchi application in the present case is given in Fig. 2.

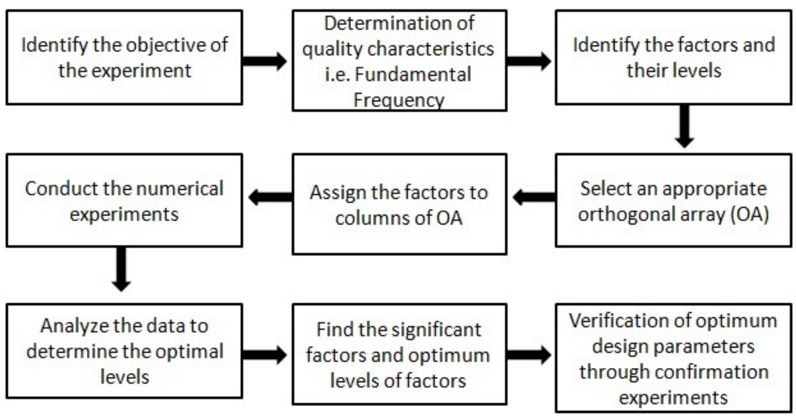

Figure 2: Steps of Taguchi approach followed in current study.

The aim of this investigation was to maximize the fundamental frequency of graphite-epoxy cylindrical shell panel having stiffeners and cutout (Fig. 3). Here, a,b are length and width of panel; h is the shell thickness; $a^{/}$, $b^{/}$ are length and width of cutout; and h_s, w_s denote thickness and width of stiffeners. The study considers four input parameters or design factors, viz., fiber direction (θ deg.), width-to-thickness ratio ((b/h), level of orthotropy of the composite (E_{11}/E_{22}) and location of the cutout centre ($\bar{x}$, $\bar{y}$). Here, non-dimensional coordinate of cutout center is given by $\bar{x}$= x/a, $\bar{y}$= y/a. Each design factor is systematically examined at three different variations to understand their effects on fundamental frequency.

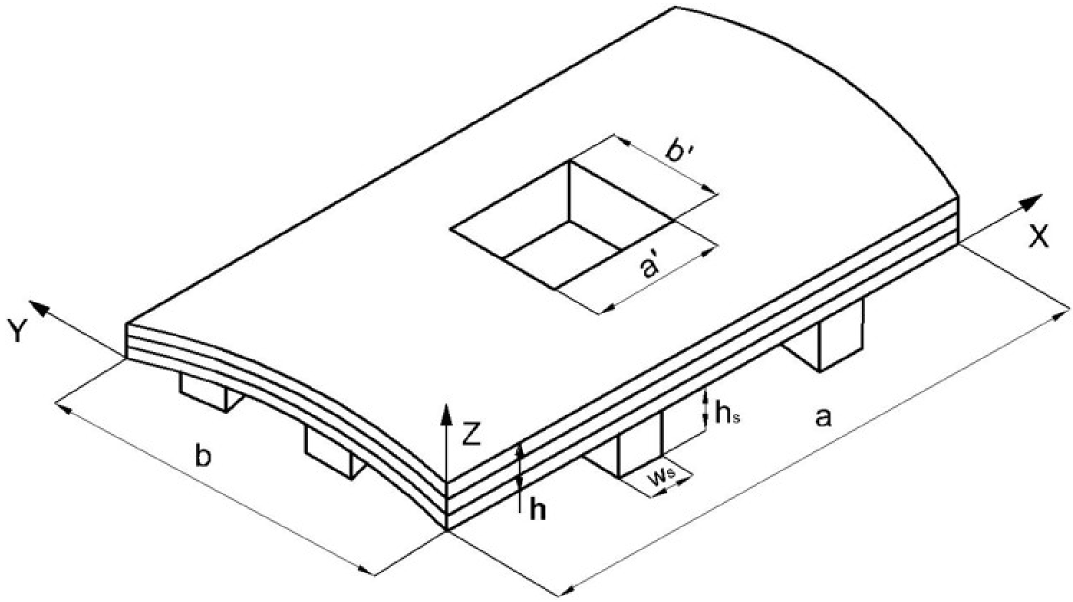

Figure 3: Composite stiffened cylindrical shell panel with cutout.

Design parameters are considered at three levels for each as given in Table 1.

Table 1. Design factors and their levels.

Design factor	Level 1	Level 2	Level 3
Fiber orientation angle (θ deg.)	30	45	60
Width/thickness ratio (b/h)	20	50	100
Degree of orthotropy (E_{11}/E_{22})	10	25	40
Position of cutout ($\bar{x}$, $\bar{y}$)	(0.2, 0.2)	(0.3, 0.3)	(0.4, 0.4)

In Taguchi design, suitable OA is determined on the basis of degrees of freedom (DOFs). DOF of OA must surpass their total number needed for analyzing the problem. On that consideration, L27 OA was selected. Trial experiments follow the combination of design variables, as shown in Table 2.
A full factorial design for four design parameters at three levels each would require 81 trials, while L27 OA only needs 27 runs. That is the advantage of using this Taguchi OA.
Next, free vibration frequency of stiffened composite cylindrical shell panels with cutout was obtained for the combination of design factors (Table 2), following a numerical scheme based on FE analysis.

Table 2. Numerical trial layout for L27 OA.

Trial No.	θ	b/h	E_{11}/E_{22}	$(\bar{x}, \bar{y})$	Trial No.	θ	b/h	E_{11}/E_{22}	$(\bar{x}, \bar{y})$
1	30	20	10	(0.2, 0.2)	15	45	50	40	(0.3, 0.3)
2	30	20	25	(0.3, 0.3)	16	45	100	10	(0.2, 0.2)
3	30	20	40	(0.4, 0.4)	17	45	100	25	(0.3, 0.3)
4	30	50	10	(0.3, 0.3)	18	45	100	40	(0.4, 0.4)
5	30	50	25	(0.4, 0.4)	19	60	20	10	(0.4, 0.4)
6	30	50	40	(0.2, 0.2)	20	60	20	25	(0.2, 0.2)
7	30	100	10	(0.4, 0.4)	21	60	20	40	(0.3, 0.3)
8	30	100	25	(0.2, 0.2)	22	60	50	10	(0.2, 0.2)
9	30	100	40	(0.3, 0.3)	23	60	50	25	(0.3, 0.3)
10	45	20	10	(0.3, 0.3)	24	60	50	40	(0.4, 0.4)
11	45	20	25	(0.4, 0.4)	25	60	100	10	(0.3, 0.3)
12	45	20	40	(0.2, 0.2)	26	60	100	25	(0.4, 0.4)
13	45	50	10	(0.4, 0.4)	27	60	100	40	(0.2, 0.2)
14	45	50	25	(0.2, 0.2)					

Numerical procedure using finite element analysis

Composite cylindrical shell has uniform thickness (h), as shown in Fig. 3. The shell consists of thin lamina each placed at an angle (θ) to the x-axis. Features such as strain-displacement equation, constitutive relation, generation of stiffness and mass matrices, modeling of cutout, etc., have been provided in details elsewhere [13]. Stiffener formulation requires consideration of a shear correction factor of 5/6. The role of eccentricity of the stiffeners in the shell was suitably considered by obtaining the section parameter values at its middle layer. Connectivity matrix takes care of the coordination between nodes of stiffener and shell. Following general FE procedure, stiffness and mass matrices at the element level were obtained first, and then those were suitably assembled to obtain global matrices. Appropriate matrices of the shell and that of stiffeners were harmonized properly to obtain the shell mass matrix. Accordingly, a global mass matrix [M] and global stiffness matrix [K] were obtained. Natural frequencies were then obtained from the condition stated in Eq. (1):

$$\left|[K] - \omega^2 [M]\right| = 0 \tag{1}$$

Subspace iteration algorithm was employed to solve this Eigenvalue problem, considering relevant boundary conditions. Normalized fundamental frequency is obtained as:

$$\bar{\omega} = \omega\, a^2 (\rho \,/\, E_{22} h^2)^{\frac{1}{2}} \tag{2}$$

where ρ represents material density.

Validation of formulation for both stiffener and cutout was checked by comparing results from FE code with benchmark results. The same was already presented elsewhere, while considering parametric behavior of cylindrical shell panels under free vibration [13].

In the present study, eight different boundary conditions on all four sides were investigated. Edge support conditions were described using terms like clamped support (C), free end (F) and simply supported (S), listed in a counterclockwise sequence starting from boundary at x=0. Accordingly, eight boundary conditions were designated as CCCC, CSCS, CSSC, FCCF, FCFC, FSFS, FSSF and SSSS, as shown in Fig. 4.

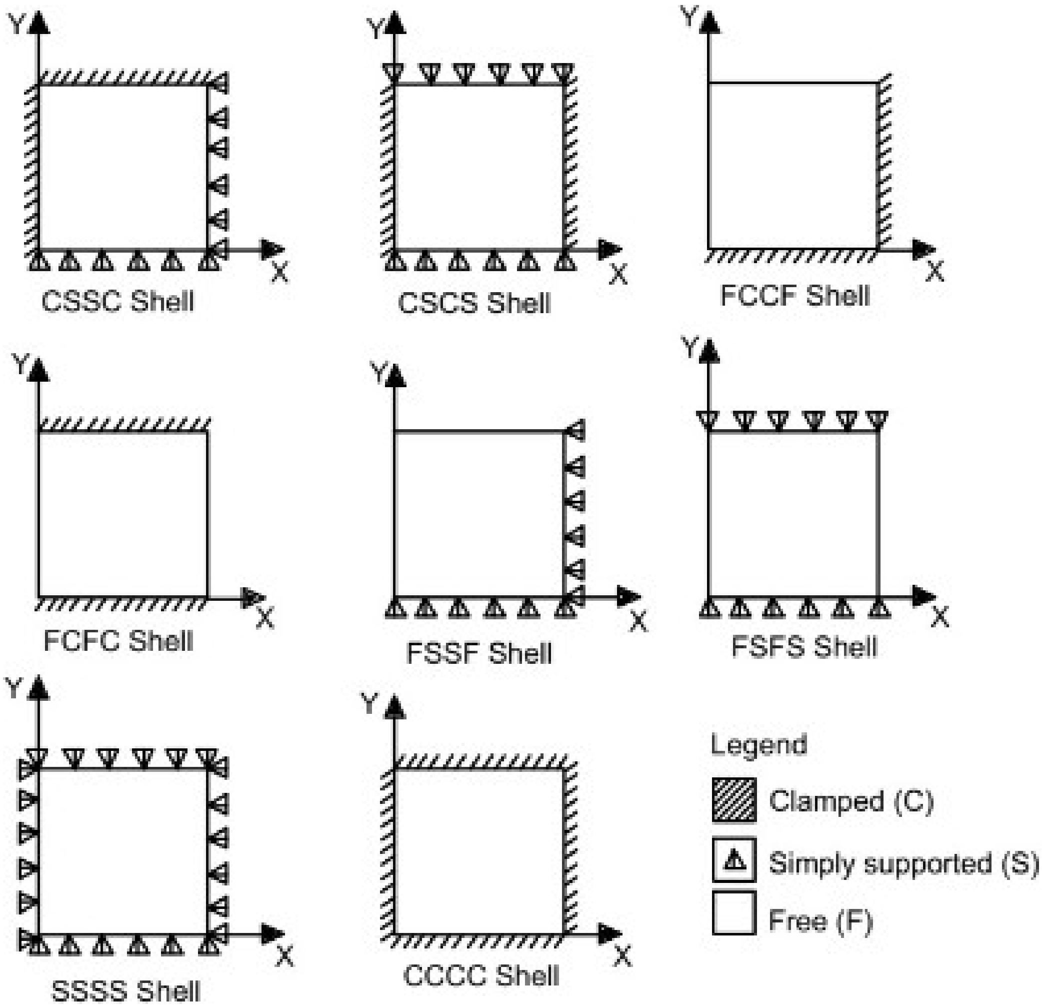

Figure 4: Arrangement of boundary conditions.

A 20-layer anti-symmetric angle-ply laminate, i.e., $[(\theta/-\theta)_{10}]$ lay-up shell was considered. Location of cutout was adjusted in relation to one end of the shell. Geometrical parameters were herein considered as: a/b = 1, a/h = 100, $a^{/}/b^{/}$ = 1, $a^{/}/a = 0.2$, h/R_y = 1/300. Material properties were listed as: $G_{13} = G_{12} = 0.5E_{22}$, $G_{23} = 0.2E_{22}$, $\nu_{12} = \nu_{21} = 0.25$.

To consider parametric variation: fiber orientation angle (θ) was varied as 30^0, 45^0, 60^0; degree of orthotropy (E_{11}/E_{22}) was varied as 10, 25, 40; width/thickness ratio (b/h) was varied as 20, 50, 100; and position of cutout center was varied as (0.2, 0.2), (0.3, 0.3) and (0.4, 0.4). Accordingly, non-dimensional fundamental frequency ($\overline{\omega}$) was obtained. Then, S/N ratio analysis was accomplished using Minitab [26]. In order to maximize fundamental frequency, larger-the-better condition had to be adopted. S/N ratios for frequency data were obtained from the following expression (n is no of test runs, y_i is frequency data):

$$\frac{S}{N} = -10\log\left[\frac{1}{n}\sum\left(\frac{1}{y_i^2}\right)\right] \tag{2}$$

Using this expression, S/N ratios were calculated for fundamental frequency data obtained by the numerical scheme based on FE formulation of the laminated cylindrical shell panel with cutout and stiffeners, by employing different practical non-uniform edge conditions. Based on those S/N ratios, Taguchi optimization was carried out to identify significant control parameters and the quantum of their significance.

Results and discussion

Results for fundamental frequencies of the cutout borne shell panel under eight practical edge conditions were obtained. However, for brevity, detailed discussion was kept restricted to specific cases, viz., CCCC and FSFS boundary conditions, as presented below.

CCCC boundary condition

Results for fundamental frequencies on CCCC shell and related S/N ratios are given in Table 3.

Table 3: Normalized fundamental frequency and S/N ratios for CCCC shell.

Trial No.	$\bar{\omega}$	S/N ratio	Trial No.	$\bar{\omega}$	S/N ratio
1	18.63	25.4	15	19.17	25.7
2	26.69	28.5	16	8.75	18.8
3	32.13	30.1	17	13.84	22.8
4	12.83	22.2	18	18.55	25.4
5	19.43	25.8	19	16.88	24.5
6	23.06	27.3	20	22.12	26.9
7	12.16	21.7	21	26.04	28.3
8	15.67	23.9	22	9.16	19.2
9	20.60	26.3	23	13.64	22.7
10	17.28	24.8	24	17.57	24.9
11	24.14	27.7	25	8.38	18.5
12	28.09	29.0	26	13.32	22.5
13	11.37	21.1	27	7.27	17.2
14	15.00	23.5			

Mean S/N ratios for each level are presented in Table 4. A higher S/N ratio suggested less variance of the fundamental frequency towards the desired target, signifying better performance. From the table, it is observed that fiber orientation angle at level 1, width/thickness ratio at level 1, degree of orthotropy at level 3, and position of cutout at level 3 (i.e., fiber orientation angle at 30^0, width/thickness ratio at 20, degree of orthotropy at 40, and position of cutout at (0.4, 0.4)) were the conditions that yielded the highest value of fundamental frequency.

Response table also represents delta value for each design factor. Design factors were then ranked based on delta value to evaluate their impact on fundamental frequency. Accordingly, width/thickness parameter is ranked 1, degree of orthotropy is ranked 2, fiber orientation angle is ranked 3 and cut-out location is ranked 4. Factor width/thickness has the major influence on determining fundamental frequency at CCCC condition.

Table 4: Response data table for CCCC shell.

Level	θ	b/h	E_{11}/E_{22}	$(\bar{x}, \bar{y})$
1	25.68	27.25	21.83	23.93
2	24.29	23.58	24.87	24.41
3	23.21	22.35	26.48	24.84
Delta	2.47	4.89	4.65	0.91
Rank	3	1	2	4

Main effect plots are commonly used to visualize the impact of different factors on the response variable, since it allows seeing at a glance which factor levels contribute most in improving the response variable. Factors with higher average S/N ratios values indicate a more significant effect on the response variable. Main effect plots for S/N ratios were derived from information in Table 3. In Fig. 5, decreasing trend of S/N ratios with fiber orientation angle and width/thickness parameter can be observed. However, an increasing trend of S/N ratios with degree of orthotropy and position of cutout can be observed. The trend is clear and definite for all parameters.

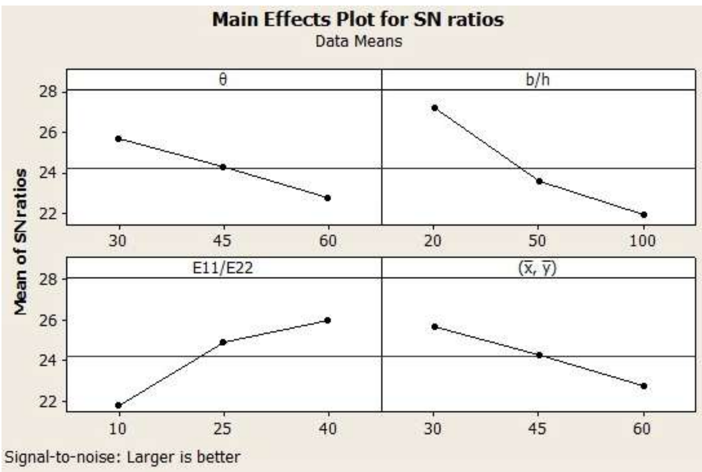

Figure 5: Main effects plot for S/N ratios for CCCC shell.

ANOVA is commonly used to assess the importance of different factors, and their interactions on the response variable. ANOVA was carried out using MINITAB 16 software to assess the impact of design parameters on the response in Taguchi's optimization method. Table 5 presents outcomes of ANOVA conducted on fundamental frequency for CCCC shell. The significance of a factor or interaction is determined using F value. A higher F value indicates a more substantial impact. In the case of CCCC shells, factor E_{11}/E_{22} attained highest F-ratio value. Factor b/h and b/h * b/h also followed a similar trend. If 'P' value was below 0.05, associated factor was considered to have a relevant influence on the response at a 95% confidence level. On reviewing 'P' values, it was noted that majority parameters had greater influence on the response except θ, θ*θ and $(\bar{x}, \bar{y})*(\bar{x}, \bar{y})$. Determination factor ($R^2$) measures how well the model fits the data. With a value of 99.82%, well above 80%, it means the model explains at least 99.82% of the variability in response data. This high R^2 suggests that the proposed model is suitable.

Table 5: ANOVA Table for CCCC shell.

Source	DF	Seq SS	Adj SS	Adj MS	F	P
θ	1	121.78	0.00	0.0039	0.024	0.879175
b/h	1	485.27	47.76	47.7613	297.512	0.000000
E_{11}/E_{22}	1	329.73	47.99	47.9904	298.939	0.000000
$(\bar{x}, \bar{y})$	1	17.60	2.27	2.2744	14.168	0.002701
θ * θ	1	0.19	0.19	0.1896	1.181	0.298455
b/h * b/h	1	42.81	42.81	42.8090	266.663	0.000000
E_{11}/E_{22}* E_{11}/E_{22}	1	7.25	7.25	7.2453	45.132	0.000021
$(\bar{x}, \bar{y})$* $(\bar{x}, \bar{y})$	1	0.25	0.25	0.2454	1.528	0.240005
θ * b/h	1	4.14	6.48	6.4828	40.382	0.000036
θ * E_{11}/E_{22}	1	20.57	27.90	27.9031	173.812	0.000000
θ *$(\bar{x}, \bar{y})$	1	0.68	4.29	4.2874	26.707	0.000234
b/h * E_{11}/E_{22}	1	25.86	25.86	25.8554	161.057	0.000000
b/h *$(\bar{x}, \bar{y})$	1	12.71	12.71	12.7095	79.169	0.000001
E_{11}/E_{22}*$(\bar{x}, \bar{y})$	1	5.30	5.30	5.3011	33.021	0.000092
Error	12	1.93	1.93	0.1605		
S = 0.400669 R-Sq = 99.82%						

Residual plots for S/N ratios help in checking if any model assumptions are proper. They spot outliers and influential points that affect the model's accuracy. By verifying the randomness of residuals, they ensure a good model fit. Residual plots also guide model improvements.

Fig. 6 confirms the model's accuracy by showing a straight-line alignment between predicted values and data from numerical analysis. Fig. 6 shows that the residual plot against fitted values of frequency does not exhibit a distinct pattern. To evaluate data independence further, residuals were plotted in contrast with testing order. Residuals plot verifies the absence of any discernible predictive pattern, with all residuals scattered within acceptable limits.

Confirmatory tests were performed to confirm optimal results obtained from Taguchi approach. The primary aim of the test is to calculate the percentage enhancement at the optimal condition with respect to initial test condition. The equation below was utilized to calculate S/N ratio for the predicted condition.

$$\bar{\eta} = \eta_m + \sum_{k=1}^{p}(\overline{\eta_k} - \eta_m) \qquad (3)$$

where overall mean data of S/N ratio is represented as η_m, mean data of S/N ratio at the optimal combination of each parameter is denoted as $\overline{\eta_k}$ and the number of design factors is denoted as 'p'.

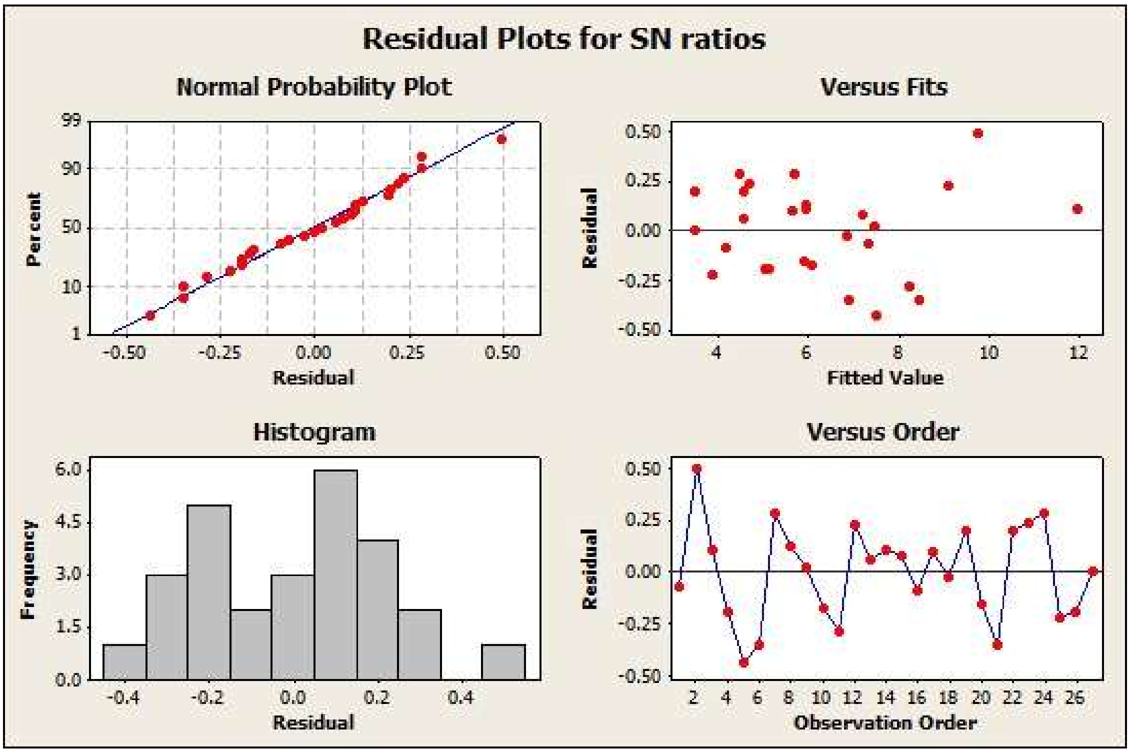

Figure 6: Residual plots for S/N ratios for CCCC shell.

Table 6 shows results of the confirmatory test for CCCC boundary conditions. S/N ratio was improved by 6.17 dB (25.78%) with respect to the initial condition. Thus, the present procedure yields substantial improvement.

Table 6: Confirmation test results for CCCC boundary condition.

Level	Initial test condition θ = 45, b/h = 50, E_{11}/E_{22} = 25, ($\bar{x}$, $\bar{y}$) = (0.3, 0.3)	Predicted condition θ = 30, b/h = 20, E_{11}/E_{22} = 40, ($\bar{x}$, $\bar{y}$) = (0.4,0.4)	FE simulation θ = 30, b/h = 20, E_{11}/E_{22} = 40, ($\bar{x}$, $\bar{y}$) = (0.4, 0.4)
ω	15.72		32.13
S/N ratio	23.93	27.42	30.10

The two-way interaction plot for CCCC condition is represented in Fig. 7.
Interaction plot for S/N ratios indicates that the effect of one factor on the response variable depends on the level of another factor.
Intersecting lines in this plot display the occurrence of substantial interaction, and non-parallel lines indicate some level of interaction. From Fig. 8, significant interaction can be found for the case of (θ * E_{11}/E_{22}) and for the rest, some levels of interactions were found.

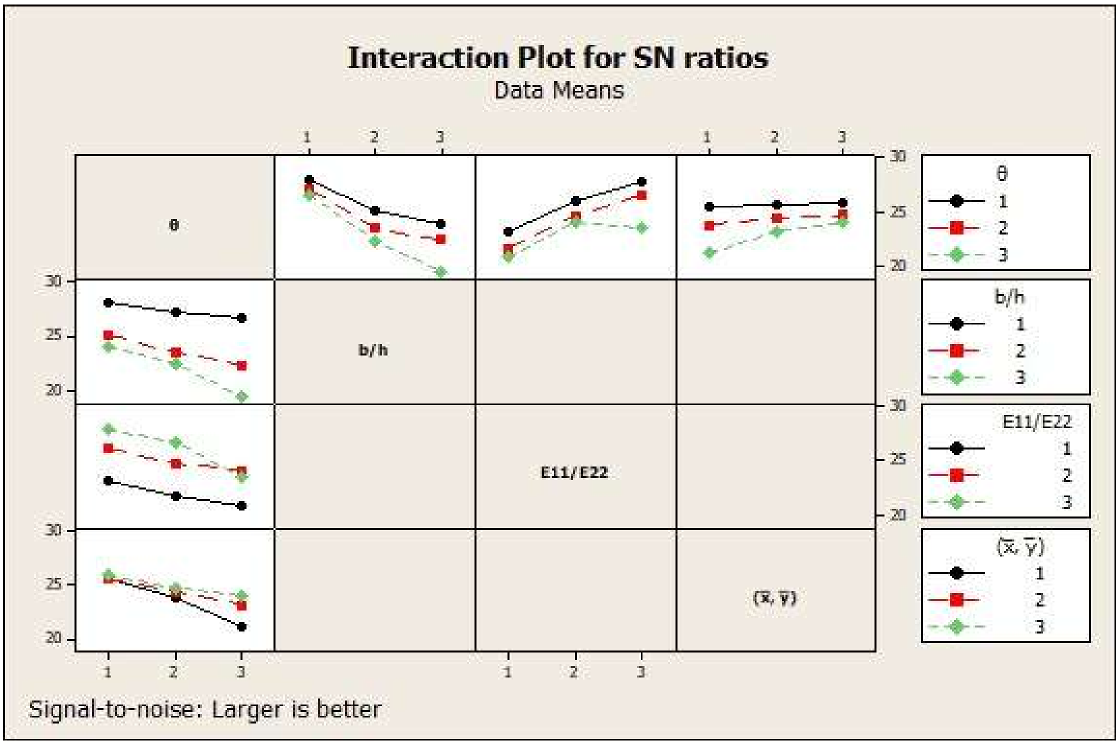

Figure 7: Interaction plots for S/N ratio for CCCC shell.

FSFS boundary condition

Results of fundamental frequencies for FSFS shell and S/N ratios are given in Table 7.

Table 7: Normalized fundamental frequency and S/N ratios for FSFS shell.

Trial No.	$\bar{\omega}$	S/N ratio	Trial No.	$\bar{\omega}$	S/N ratio
1	7.3	17.2	15	7.3	17.3
2	10.3	20.2	16	4.1	12.2
3	12.1	21.6	17	5.7	15.2
4	4.9	13.8	18	6.8	16.7
5	7.1	17.0	19	4.8	13.6
6	8.1	18.2	20	5.8	15.2
7	4.7	13.5	21	6.6	16.4
8	6.1	15.6	22	3.7	11.4
9	7.5	17.5	23	4.9	13.9
10	5.9	15.4	24	6.0	15.5
11	8.0	18.0	25	3.6	11.2
12	9.3	19.4	26	7.3	17.2
13	4.6	13.3	27	10.3	20.2
14	6.1	15.6			

Response table for S/N ratios highlights mean values in Table 8. Analysis reveals that maximum $\bar{\omega}$ was achieved under specific parametric conditions: fiber orientation angle at level 1, width/thickness ratio at level 1, degree of orthotropy at level 3, and position of cutout at level 3 (i.e., fiber orientation angle of 30^0, width/thickness ratio of 20, degree of orthotropy of 40, and a cutout position of

(0.4, 0.4)). Response table also provides delta value for each design factor. Looking at Table 8, fiber orientation angle is ranked 1, degree of orthotropy is ranked 2, width/thickness parameter is ranked 3 and cut-out location is ranked 4. So, according to this ranking, fiber orientation angle has the most significant influence on determining fundamental frequency for FSFS shell.

Table 8: Response data table for FSFS shell.

Level	θ	b/h	E_{11}/E_{22}	$(\bar{x}, \bar{y})$
1	17.19	17.45	13.51	15.07
2	15.9	15.1	16.05	15.65
3	13.51	14.05	17.03	15.88
Delta	3.68	3.39	3.52	0.81
Rank	1	3	2	4

Main effects' plot for FSFS boundary conditions is shown in Fig. 8. A similar trend is found as in CCCC boundary condition. The plot shows that the best condition for highest fundamental frequency is when lamination angle is 30^0, width/thickness ratio is 20, degree of orthotropy is 40, and cutout is positioned at (0.4, 0.4).

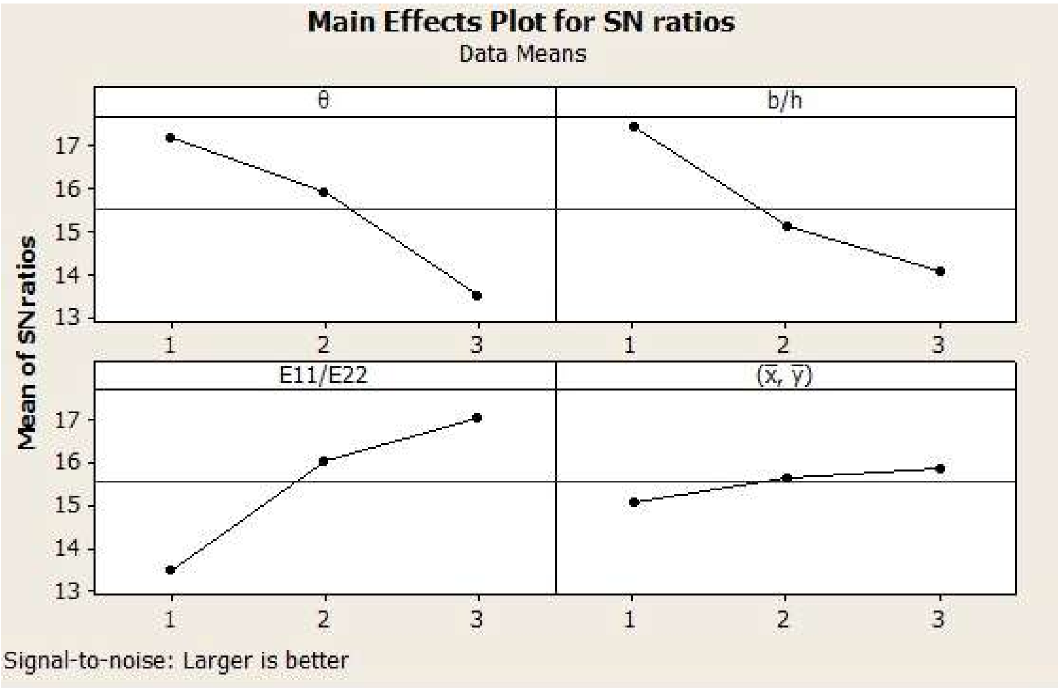

Figure 8: Main effects plot for S/N ratios for FSFS shell.

Results of ANOVA for FSFS shell are shown in Table 9. In the case of FSFS shell, factor E_{11}/E_{22} attains highest F-ratio value followed by b/h. Major combinations are significant at 95% confidence level, while few combinations are less significant on the response at this level. High determination factor (R^2) suggests that the proposed model is suitable.

Table 9: ANOVA Table for FSFS shell.

Source	DF	Seq SS	Adj SS	Adj MS	F	P
θ	1	32.805	0.033	0.03274	0.2890	0.600712
b/h	1	29.338	4.663	4.66311	41.1526	0.000033
E_{11}/E_{22}	1	30.681	4.802	4.80219	42.3800	0.000029
$(\bar{x}, \bar{y})$	1	1.434	0.153	0.15334	1.3532	0.267324
θ * θ	1	0.299	0.299	0.29927	2.6411	0.130091
b/h * b/h	1	2.407	2.407	2.40667	21.2392	0.000602
E_{11}/E_{22}* E_{11}/E_{22}	1	0.821	0.821	0.82140	7.2490	0.019583
$(\bar{x}, \bar{y})$* $(\bar{x}, \bar{y})$	1	0.010	0.010	0.00960	0.0847	0.775968
θ * b/h	1	3.203	2.193	2.19343	19.3573	0.000866
θ * E_{11}/E_{22}	1	3.876	4.238	4.23814	37.4022	0.000052
θ *$(\bar{x}, \bar{y})$	1	0.002	0.162	0.16200	1.4297	0.254911
b/h * E_{11}/E_{22}	1	2.048	2.048	2.04800	18.0739	0.001125
b/h *$(\bar{x}, \bar{y})$	1	0.372	0.372	0.37174	3.2806	0.095190
E_{11}/E_{22}*$(\bar{x}, \bar{y})$	1	1.016	1.016	1.01550	8.9620	0.011198
Error	12	1.360	1.360	0.11331		
S = 0.325687 R-Sq = 97.84%						

In Fig. 9, the graph shows that predictions match actual data well. All dots in the plot form a straight line, which is a good sign.

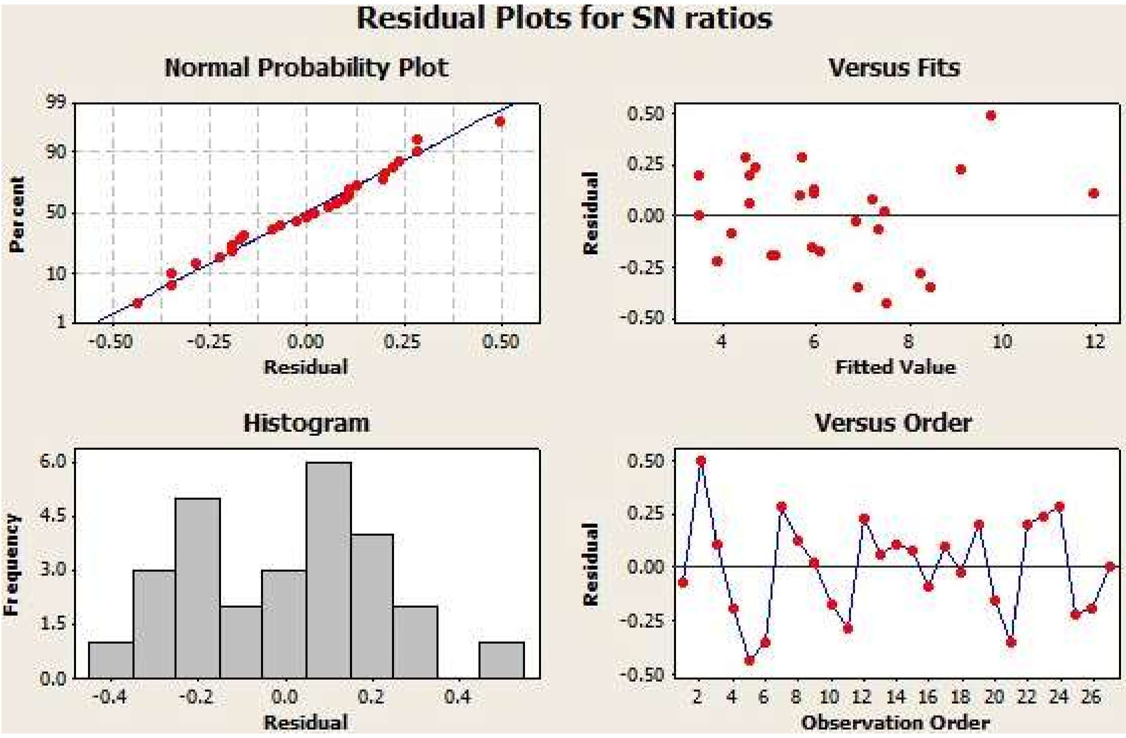

Figure 9: Residual plots for S/N ratios for FSFS shell.

Plot of residuals *vs*. prediction does not show any specific pattern. Two-way interaction plot for FSFS condition is represented in Fig. 10. Intersecting lines in this plot reveal the presence of significant interaction, and non-parallel lines indicate some level of interaction. From Fig. 10, significant interactions are for combination of (θ * E_{11}/E_{22}) and (θ * $(\bar{x}, \bar{y})$).

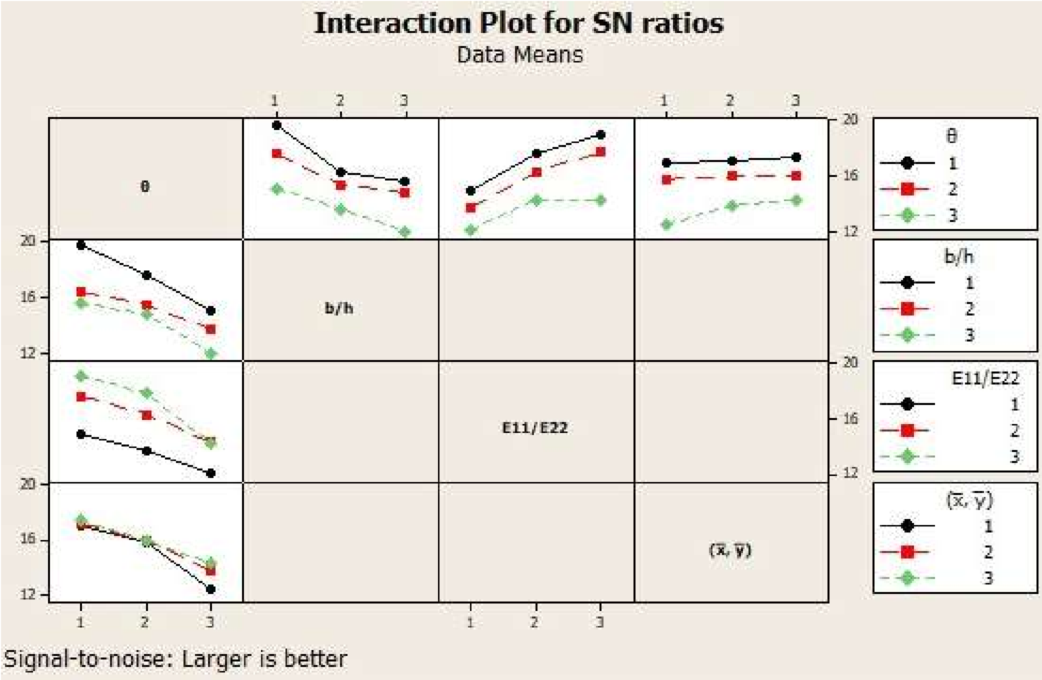

Figure 10: Interaction plot for S/N ratio for FSFS shell.

Table 10 shows results of the confirmatory test for FSFS boundary conditions. S/N ratio is improved by 5.78 dB (36.53%) compared to initial condition. Thus, the present procedure yields considerable improvement.

Table 10: Confirmation test results for CCCC boundary condition.

Level	Initial test condition θ = 45, b/h = 50, E_{11}/E_{22} = 25, $(\bar{x}, \bar{y})$ = (0.3, 0.3)	Predicted condition θ =30, b/h = 20, E_{11}/E_{22} =40, $(\bar{x}, \bar{y})$ = (0.4,0.4)	FE Simulation θ = 30, b/h = 20, E_{11}/E_{22} =40, $(\bar{x}, \bar{y})$ = (0.4, 0.4)
ω	6.18		12.10
S/N ratio	15.82	18.61	21.60

Other boundary conditions

Similar analysis was conducted for other boundary conditions as well, but details are omitted here for brevity. Optimal conditions for achieving maximum fundamental frequency under all eight boundary conditions are summarized in Table 11.

Table 11: Optimum condition at different boundary conditions.

Shell boundary	θ	b/h	E_{11}/E_{22}	$(\bar{x}, \bar{y})$
CCCC	30	20	40	(0.4, 0.4)
FSFS	30	20	40	(0.4, 0.4)
CSCS	30	20	40	(0.4, 0.4)
CSSC	45	20	40	(0.4, 0.4)
FCCF	30	20	40	(0.4, 0.4)
FCFC	30	20	40	(0.4, 0.4)
FSSF	45	20	40	(0.4, 0.4)
SSSS	45	20	40	(0.4, 0.4)

Largest fundamental frequencies are identified at lower level of width/thickness parameter, higher level of degree orthotropy and higher level of position of cutout for all boundary conditions. Fiber orientation angle plays a distinct role in deciding maximum fundamental frequency of composite cylindrical shell for varying boundary conditions.

Conclusions

In this study, free vibration frequencies of cutout borne stiffened composite cylindrical shells were determined using FE based numerical procedure. Taguchi analysis was then used to maximize fundamental frequency. Optimum combination of shell parameters was obtained under various practical boundary conditions. Analysis of variance (ANOVA) reveals significant shell parameters for each of the boundary conditions. The following conclusions are drawn: highest fundamental frequencies were noticed at a lower width/thickness ratio (b/h = 20) and higher degrees of orthotropy (E_{11}/E_{22}= 40) and cutout position (0.4, 0.4) for all boundary conditions; fiber orientation angle played a distinct role in deciding maximum fundamental frequency for varying boundary constraints; width/thickness ratio strongly affected fundamental frequency in different boundary conditions- it is followed by degree of orthotropy, fiber orientation angle, and position of cutout in descending order of impact; values of determination factor (R^2) for all models are greater than 80%, which indicates that the proposed model is adequate.

It is envisaged that the present results regarding optimum design conditions will help practicing engineers and designers dealing with such laminated composite shell panels in deciding the proper positioning of the cutout and stiffeners depending on boundary constraints.

Authors’ contributions

Sudip Kr. Halder: Data generation; formal analysis; review of literature; preparation of first draft. **Anirban Mitra**: Review of literature; data analysis; review of first draft. **Sarmila Sahoo**: Review of literature; formulation; data analysis; review and editing of first draft.

Abbreviations

ANOVA: analysis of variance
C: clamped support
DOE: design of experiments
DOF: degrees of freedom
F: free edge
FE: finite element
OA: orthogonal array
S: simply supported edge
S/N: signal-to-noise ratio

References

1. Zhang L, Zhao L, Pan L et al. Research progress of composite cylindrical shells. Polym Comp. 2023;44(11):7298-7316. https://doi.org/10.1002/pc.27659
2. Sahoo S. Design Aids for Stiffened Composite Shells with Cutouts. Springer Singapore. 2017. https://doi.org/10.1007/978-981-10-2062-9
3. Leissa AW, Lee JK, Wang AJ. Vibrations of cantilevered shallow cylindrical shells of rectangular planform. J Sound Vib. 1981;78(3):311-28. https://doi.org/10.1016/S0022-460X(81)80142-3
4. Chung H. Free vibration analysis of circular cylindrical shells. J Sound Vib. 1981;74(3):331-50. https://doi.org/10.1016/0022-460X(81)90303-5
5. Soldatos KP. Free vibrations of antisymmetric angle-ply laminated circular cylindrical panels. Q J Mech Appl Math. 1983;36(2):207-21. https://doi.org/10.1093/qjmam/36.2.207
6. Lim CW, Liew KM. A higher order theory for vibration of shear deformable cylindrical shallow shells. Int J Mech Sci. 1995;37(3):277-95. https://doi.org/10.1016/0020-7403(95)93521-7
7. Naeem MN, Sharma CB. Prediction of natural frequencies for thin circular cylindrical shells. Proc Inst Mech Eng, Part C: J Mech Eng Sci. 2000;214(10);1313-28. https://doi.org/10.1243/0954406001523290
8. Zhang XM, Liu GR, Lam KY. Vibration analysis of thin cylindrical shells using wave propagation approach. J Sound Vib. 2001;239(3):397-403. https://doi.org/10.1006/jsvi.2000.3139
9. Xuebin L. Study on free vibration analysis of circular cylindrical shells using wave propagation. J Sound Vib. 2008;311(3-5):667-82. https://doi.org/10.1016/j.jsv.2007.09.023
10. Dennis ST, Palazotto AN. Static response of a cylindrical composite panel with cutouts using a geometrically nonlinear theory. AIAA J. 1990;28(6):1082-88. https://doi.org/10.2514/3.25170
11. Nanda N, Bandyopadhyay JN. Nonlinear free vibration analysis of laminated composite cylindrical shells with cutouts. J Reinf Plast Compos. 2007;26(14):1413-27. https://doi.org/10.1177/0731684407079776
12. Chakravorty D, Sinha PK, Bandyopadhyay JN. Applications of FEM on free and forced vibration of laminated shells. J Eng Mech. 1998;124(1):1-8. https://doi.org/10.1061/(ASCE)0733-9399(1998)124:1(1)
13. Sahoo S. Laminated composite stiffened cylindrical shell panels with cutouts under free vibration. Int J Manuf Mater Mech Eng. 2015;5(3):37-63. https://doi.org/10.4018/IJMMME.2015070103
14. Khosravi AE, Shahabian F, Aftabi Sani A. Free vibration of cylindrical shells and panels with cutout via the differential transform method. Mech Adv Mater Struct. 2023;1-19. https://doi.org/10.1080/15376494.2023.2294494

15. Savine F, Irisarri FX, Julien C et al. A component-based method for the optimization of stiffener layout on large cylindrical rib-stiffened shell structures. Struct Multidiscip Optim. 2021;64(4):1843-61. https://doi.org/10.1007/s00158-021-02945-9
16. Guo C, Liu T, Wang Q et al. Spectral-Tchebychev technique for the free vibration analysis of composite laminated stepped and stiffened cylindrical shells with arbitrary boundary conditions. Compos Struct. 2021;272:114193. https://doi.org/10.1016/j.compstruct.2021.114193
17. Talezadehlari A. Free vibration analysis of perforated composite cylindrical shell and panel using multi-domain generalized differential quadrature (GDQ) method. Compos Struct. 2022;287:115337. https://doi.org/10.1016/j.compstruct.2022.115337
18. Bakulin VN, Boitsova DA, Nedbai AY. Parametric resonance of a three-layered cylindrical composite rib-stiffened shell. Mech Compos Mater. 2021;57:623-34. https://doi.org/10.1007/s11029-021-09984-9
19. Chaudhuri PB, Mitra A, Sahoo S. A parametric study of higher-mode natural frequencies of composite stiffened cylindrical shell with cut-out. Eng Trans. 2023;71(1):81-109. https://doi.org/10.24423/EngTrans.2456.20230126
20. Choudhary PK. Optimal design of composite cylindrical shells subject to compression buckling strength. Multidiscip Model Mater Struct. 2023;19(5):829-47. https://doi.org/10.1108/MMMS-11-2022-0269
21. Shinde Bharti M, Sayyad Atteshamuddin S. Bending analysis of laminated composite cylindrical shell using fifth order shear deformation theory. In Fiber Reinforced Polymeric Materials and Sustainable Structures. Singapore: Springer. 2023:235-242. https://doi.org/10.1007/978-981-19-8979-7_19
22. Cho HK. Optimization of laminated composite cylindrical shells to maximize resistance to buckling and failure when subjected to axial and torsional loads. Int J Precis Eng Manuf. 2018;19:85-95. https://doi.org/10.1007/s12541-018-0010-6
23. Mohammadrezazadeh S, Jafari AA. Nonlinear vibration suppression of SS and CC laminated composite cylindrical shells with magnetostrictive strips. Mech Based Des Struct Mach. 2023;51(10):5470-91. https://doi.org/10.1080/15397734.2021.2004163
24. Taguchi G. Introduction to Quality Engineering. Asian Productivity Organization: Tokyo. 1990.
25. Montgomery DC. Design and Analysis of Experiments. Wiley: New York. 2001.
26. Minitab User Manual (Release 13.2). Making Data Analysis Easier. MINITAB Inc., State College: PA, USA. 2001.